Water Practice & Technology Vol 16 No 2
doi: 10.2166/wpt.2021.006

Statistical analysis of fine resolution flow datasets helps characterizing flow behaviour in primary clarifiers: a decision support method

Katalin Kiss[a,*] and Miklós Patziger[b]

[a] Department of Sanitary and Environmental Engineering, Budapest University of Technology and Economics, Mu˝egyetem rkp. 1-3., H-1111, Budapest, Hungary

[b] Department of Sanitary and Environmental Engineering, Budapest University of Technology and Economics, Budapest, Hungary

*Corresponding author. E-mail: kiss.katak@gmail.com

Abstract

In situ measurement campaigns of primary clarifiers are rarely implemented properly because of their cost, time, and energy demand. Hydrodynamic modelling possibilities for such reactors have been intensely examined recently, but on-site factors affecting flow characteristics (e.g. flow distributors) have not received sufficient attention. This paper describes the use of ANOVA in examining fine resolution flow datasets and the related decision support method for *in situ* measurement campaigns and subsequent modelling processes. The characteristics of the flow and the applicability of 2D and 3D methods to investigate hydrodynamic features are discussed through the example of a rectangular primary clarifier, also considering the reproducibility of measurements ranging from typical nominal flow rates to peak loads. Based on the data, recommendations are provided on the adequate sizing of a measurement campaign, potentially reduced to a single longitudinal section (2D measurement). According to our results, performing hydrodynamic measurements with a 2D-arrangement of measuring points is sufficient in the case of such clarifiers, also with regard to the design processes. When applying the described methods, the related efforts and costs may be reduced and estimated more easily. However, care should be taken when applying this method to determine the spacing of measuring points correctly.

Key words: ANOVA, flow characteristics, flow measurement, primary clarifier

Highlights

- Uncertainties of *in situ* measurement and CFD modelling of a primary clarifier.
- Decision support method based on a statistical analysis (ANOVA) is introduced.
- A rectangular PST is examined ranging from typical nominal flow rates to peak loads.
- 2D-arrangement of measuring points (single longitudinal section) is sufficient.
- Near the bottom, the distance between measuring points should not exceed 0.3 m.

Water Practice & Technology Vol 16 No 2
doi: 10.2166/wpt.2021.006

Graphical Abstract

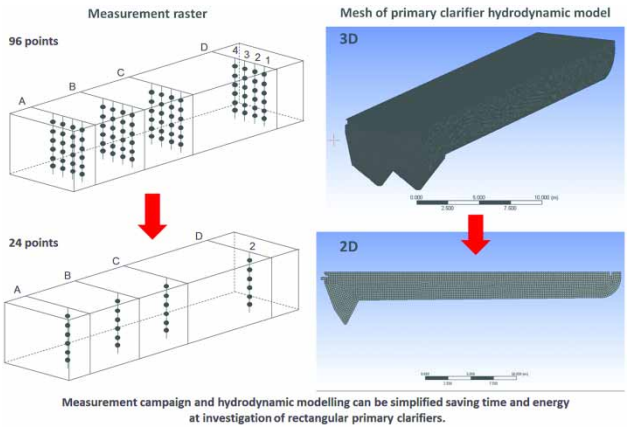

INTRODUCTION

Regarding the settling tanks used for wastewater treatment, very few references are available on the implementation of *in situ* measurement campaigns using measuring profiles; that is, vertical profiles along which flow and/or water quality are measured (Imam *et al.* 1983; Mazzolani *et al.* 1998; Ekama & Marais 2000; Patziger 2007; Burt 2010; Ramin *et al.* 2014; Patziger & Kiss 2015; Das *et al.* 2016). Campaigns including repeated measurements for a given reactor at identical or different loads are even less frequently implemented. Comprehensive measurements require extra budget, time and effort regarding planning and the evaluation of data on behalf of researchers and/or designers. On the other hand, the drawing of in-depth conclusions about the hydrodynamic behaviour of the liquid in a wastewater reactor requires carefully measured datasets and their statistical evaluation regarding flow and turbulence features.

Table 1 lists some references related to flow measurements in settling tanks. In these, various solutions were applied regarding the distribution of measurement points in the tanks. Cases where measurement points were arranged on a vertical plane are referred to as having a 2D measurement scale, whereas 3D measurement scale implies the application of several planes and sections. Numbers of replicates are also indicated. Campaigns in recent years have been characterized by 3D measurement scales and an increased number of replicates under identical hydraulic conditions, presumably as a result of technological improvements.

In addition to flow measurements, modelling is another common tool that promotes the understanding of the hydraulic behaviour in wastewater treatment reactors. Modelling is also used in other types of research projects in the water management sector. Just like SSTs, PSTs may also be modelled by CFD (Computational Fluid Dynamics). While SSTs have been widely investigated, PSTs have gained less attention in this respect; however, an increasing number of research papers have been published in recent years. PSTs and SSTs have been modelled mainly in 2D (see Mazzolani *et al.* (1998), Patziger (2007), Razmi *et al.* (2009), Rostami *et al.* (2011), Shahrokhi *et al.* (2012; 2013); Ramin *et al.* (2014), Gao & Stenstrom (2018), and Valle Medina & Laurent (2020). However, some of these clarifier reactors have also been analysed in 3D, when flow distribution is needed to be described in detail including, for instance, the effects of flow distributors at the inlet structures, unequal wastewater load in the tank, or even those of the wind (Kiss 2013; Das *et al.* 2016; Gao & Stenstrom 2019a, 2019b). The application of 3D methods is usually indispensable in reactors characterized by a highly turbulent flow induced by flow generators or aerators, such as impellers or agitators i.e. in anoxic and aerobic tanks, coagulators/flocculators, fermenters, sludge conditioning tanks etc. (see Alleyne *et al.* 2014; Karpinska & Bridgeman 2016, 2017; Skáfár *et al.* 2016).

Water Practice & Technology Vol 16 No 2
doi: 10.2166/wpt.2021.006

Table 1 | References with flow measurements

Reference	Type of settling tank	Measurement scale (distribution of measurement points in the tank)	Number of replicates
Larsen (1977) (cited as data for verification by Mazzolani *et al.* (1998), Wicklein & Samstag (2008)	Rectangular ST	2D full-scale	–
Imam (1981) cited by Imam *et al.* (1983) (cited as data for verification by Rostami *et al.* (2011))	Rectangular ST	2D laboratory-scale	–
Lindeborg *et al.* (1996)	Rectangular PST	3D full-scale	–
Winkler (2001)	Rectangular SST	2D pilot-scale	2–3, depending on the conditions
Patziger (2007)	Circular SST	2D full-scale, one radial section	3
Razmi *et al.* (2009)	Rectangular PST	2D laboratory-scale	6
Burt (2010)	Circular SST	2D full-scale, one radial section	3
Shahrokhi *et al.* (2013)	Rectangular PST	2D laboratory-scale	4
Ramin *et al.* (2014)	Circular SST	3D full-scale	–
Patziger & Kiss (2015)	Rectangular PST	3D full-scale	3, for each load level
Kemper (2016)	Stormwater ST: (1) without lamellae, (2) without lamellae, but with treated water troughs and (3) with lamellae and treated water troughs	3D laboratory-scale	2–4, depending on tank properties
Gregušová *et al.* (2017)	Rectangular and circular ST	3D full-scale	Not specified

Measurement scales and numbers of replicates are indicated. ST: primary settling tank; PST or SST: secondary settling tanks.

Obviously, examining a reactor in 3D requires extended measurements and increased modelling time and computing effort. These may be saved using 2D modelling, when axial flow, symmetric flow or plug flow is assumed. Mesh generation and the number of cells in 3D modelling require massive computing power. For example, building a 3D model for a PST in a CFD environment may require as many as 4,756,653 cells and excellent mesh quality (Figure 1), while in the case of 2D models, 16,045 cells will already give satisfying mesh quality. Hence, 3D modelling presumes more sophisticated mesh design and cell geometry than 2D methods, while the latter ones are usually easier to handle and the related on-site measurements are simpler to perform.

Examinations were performed on the accuracy of *in situ* 3D flow measurements in a PST and an anoxic tank (Kiss & Patziger 2018). A useful protocol for practical *in situ* measurements using ADV (Acoustic Doppler Velocimetry) in PSTs and anoxic tanks was developed and several comparisons were made between non-filtered and filtered data series focusing on the most important turbulence features, such as TKE (turbulent kinetic energy), Tu (degree of turbulence), L_{EI} (characteristic eddy scale) and D_t (turbulent diffusion coefficient). The authors concluded that in PSTs, the filtering of measured data influenced measuring uncertainty to a lesser extent than repeating the measurements and lateral eddy diffusivity had a significant influence on turbulence features of wastewater in the tank.

The study analysed full-scale measurement datasets for a conventional rectangular PST by means of analysis of variance (ANOVA) (Bolla & Krámli 2005, 2012), applying this statistical test in a uniquely new, innovative way to quantify flow characteristics from the following aspects: (i) How to arrange

Water Practice & Technology Vol 16 No 2
doi: 10.2166/wpt.2021.006

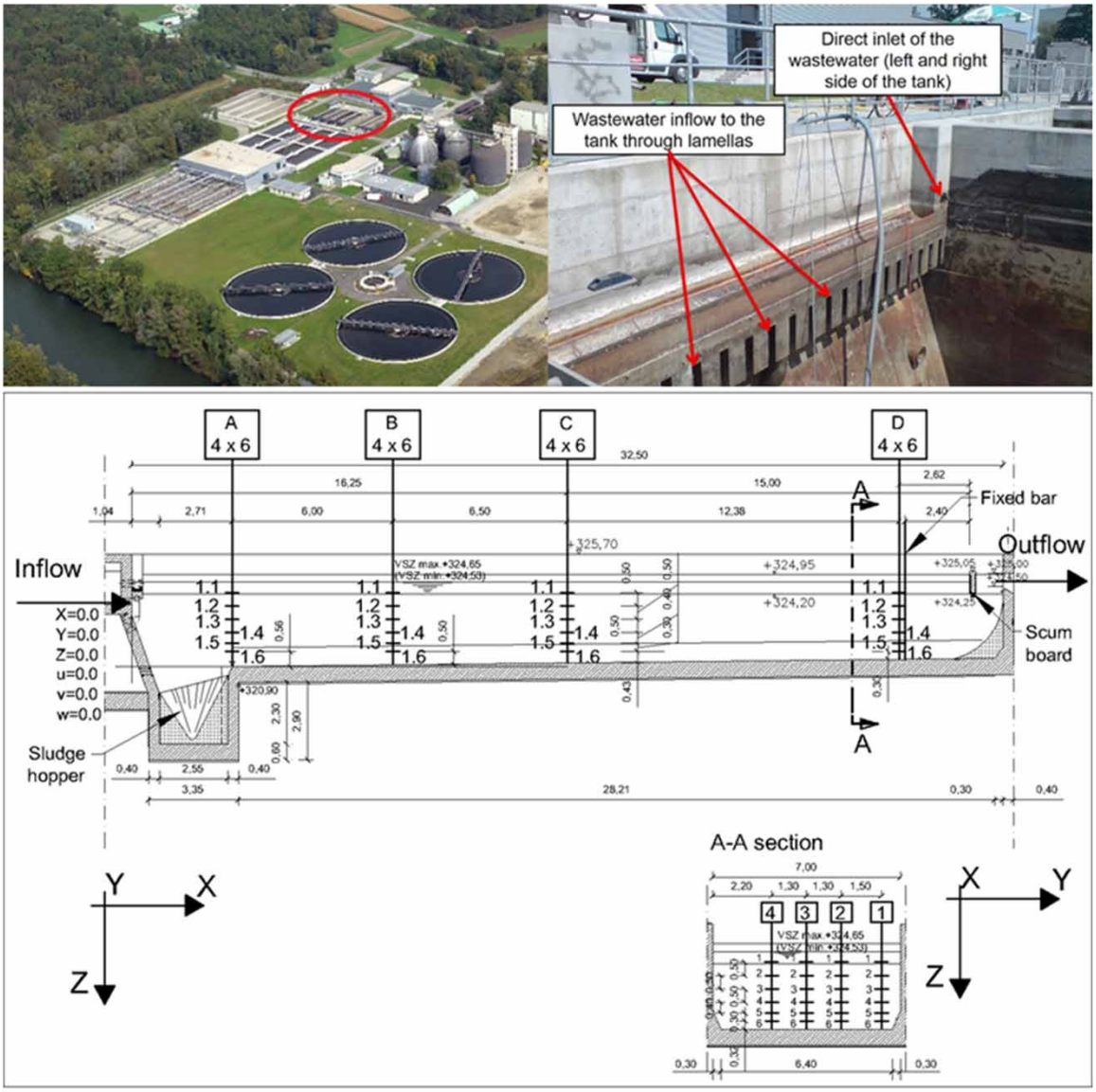

Figure 1 | Top: Location of the examined PST in the Graz WWTP and the inlet structure of the tank. Bottom: Measuring raster.

measuring points in space to describe the hydrodynamic features of the flow (2D or 3D)? (ii) Is it necessary to repeat measurements? (iii) What is the flow characteristic?

ANOVA is a widely used statistical method for the analysis of linear models, for example when planning experiments or for the purposes of quality control (Bolla & Krámli 2005, 2012). In our paper, the effects of different loads ranging from the nominal load (ATV-DVWK A 131 2016) to the peak load are discussed. Our main goal was to propose a decision support method through system analysis for the implementation of *in situ* measurement campaigns and subsequent CFD modelling. The dimensions and extent of measurements and modelling for this particular type of reactor are discussed.

METHODS

Measurement campaign

The measurement campaign (Patziger & Kiss 2015) was implemented at the Graz Municipal Wastewater Treatment Plant (Graz WWTP). The nominal capacity of the plant is 500,000 PE,

Water Practice & Technology Vol 16 No 2
doi: 10.2166/wpt.2021.006

90,000 $m^3\,d^{-1}$ with peak capacities of 1,600 $l\,s^{-1}$ and 3,200 $l\,s^{-1}$ (in dry and wet weather, respectively).

One of the four rectangular PSTs of the plant was investigated as presented by Patziger & Kiss (2015).

The tanks are 32.50 m long, 7.00 m wide and 3.95 m deep on average (Figure 1). At the front, sludge hoppers are installed under the tank inlets. Rectangular inlets are positioned high above the bottom and near the water surface. Wastewater flows into the tanks through lamellae, which dissipate its kinetic energy (Figure 1) (Patziger & Kiss 2015). Moreover, wastewater flows into the tank through circular pipes, with their openings over the water surface, on both sides. The bottom of the tanks is slightly sloped. Settled sludge is removed by a scraper and pushed towards sludge hoppers at a speed of less than 0.02 m s^{-1} to avoid disturbing settling and thickening processes at the bottom. After primary settling, wastewater leaves the tank through effluent weirs located at the back.

1.1-1.2-1.3-1.4 measurement points have 0.50 m distance from each other vertically, while between 1.4–1.5 and 1.5–1.6 points, 0.40 m and 0.30 m were in one profile, respectively (Figure 1).

To investigate hydrodynamic behaviour, the measuring method developed and successfully used for the examination of SSTs (Patziger *et al.* 2005, 2012) was adapted.

The flow pattern was analysed by ADV 'NORTEK Vector' (Nortek AS 2005), which is able to detect very low velocities and turbulence features even in the range of mm s^{-1}. Measuring points in the raster were aligned along four longitudinal sections. Sections 2 and 4 are positioned to the left and the right of Section 3, respectively, at identical distances (Figure 1) (Patziger & Kiss 2015). Measured velocity components were u, v and w belonging to the directions x, y and z, respectively. TKE values were derived from velocity variance by means of the statistical analysis of fine scale velocity data (16 s^{-1}) (Patziger & Kiss 2015).

Measurements were performed at three surface overflow rates ($q_A = 5$, 9.5 and 13 m h^{-1}) calculated as follows:

$$\boldsymbol{q_A = \frac{Q_{in}}{A_{PST}}} \tag{1}$$

where

q_A is the surface overflow rate [$m^3\,m^{-2}\,h^{-1} = m\,h^{-1}$];
Q_{in} is the inflow flow rate into the PST [$m^3\,h^{-1}$];
A_{PST} is the surface area of the PST [m^2] and
$q_A = 5$ m h^{-1}; very close to the typical design rate, 1–4 m h^{-1}.

The higher turbulence in the PST was investigated by an overflow rate of $q_A = 9.5$ and 13 m h^{-1}.

Measurements were repeated three times for each surface overflow rate, resulting in the components u1, v1, w1, u2, v2, w2, u3, v3 and w3. This solution facilitates a thorough analysis of individual load levels.

Flow distribution was investigated using the vectors calculated from u and w from the longitudinal sections 1, 2, 3 and 4. 3D images of resultant velocity vectors are also presented, providing comprehensive information on the effect of the lateral velocity components (v-components).

ANOVA

Data were analysed by 2-way ANOVA with interaction (hereinafter 2i). For the purpose of statistical analysis, data were arranged in a table according to two treatments (Bolla & Krámli 2005, 2012). Data classified according to two criteria may be arranged in $k{\cdot}p$ groups. More than one (n) observations are contained in a single cell, and an interaction is assumed between the two investigated effects

Water Practice & Technology Vol 16 No 2
doi: 10.2166/wpt.2021.006

(effects a and b). Independent, homoscedastic sample items are marked as X_{ijl} ($i = 1, \ldots, k$; $j = 1, \ldots, p$; $l = 1, \ldots, n$). The sample size is $k \cdot p \cdot n$. We assume that the linear model $X_{ijl} = \mu + a_i + b_j + c_{ij} + \varepsilon_{ijl}$ applies, where c_{ij} items are the interactions and $\varepsilon_{ij} \tilde{N}(0, \sigma^2)$ items are independent and identically distributed (i.i.d.). Normalization is calculated as:

$$\sum_{i=1}^{k} a_i = 0, \quad \sum_{j=1}^{p} b_j = 0 \tag{2}$$

$$\sum_{i=1}^{k} c_{ij} = 0 \ (j = 1, \ldots, p) \quad \text{and} \quad \sum_{j=1}^{p} c_{ij} = 0 \ (i = 1, \ldots, k) \tag{3}$$

To analyse variance (Q, the sum of the squared deviations from the mean), an ANOVA table was used (Table 2).

In the cases of $\mu \neq 0$, we presume a lack of interactions:

$$H_{0ab}: c_{ij} = 0, \ (i = 1, \ldots, k; j = 1, \ldots, p) \tag{4}$$

If the hypothesis is accepted (no interaction), our null-hypothesis will be

$$H_{0a}: a_1 = a_2 = \cdots = a_k = 0 \tag{5}$$

and

$$H_{0b}: b_1 = b_2 = \cdots = b_p = 0. \tag{6}$$

To test these hypotheses, the F-test is applied, using the following formulas:

$$\text{Below } H_{0ab} \quad F_{ab} = \frac{S_c^2}{S_e^2} \tilde{\mathcal{F}}((k-1)(p-1), kp(n-1)) \tag{7}$$

$$\text{Below } H_{0a} \quad F_a = \frac{S_a^2}{S_e^2} \tilde{\mathcal{F}}(k-1, kpn-k-p+1) \tag{8}$$

$$\text{Below } H_{0b} \quad F_b = \frac{S_b^2}{S_e^2} \tilde{\mathcal{F}}(p-1, kpn-k-p+1) \tag{9}$$

Table 2 | Equations of 2-way ANOVA with interaction (Bolla & Krámli 2005, 2012)

Cause of deviation	Sum of squares	Degree of freedom	Empirical variance
Effect a	$Q_a = pn \sum_{i=1}^{k} (\bar{X}_{i..} - \bar{X}_{...})^2$	$k-1$	$S_a^2 = \frac{Q_a}{k-1}$
Effect b	$Q_b = kn \sum_{j=1}^{p} (\bar{X}_{.j.} - \bar{X}_{...})^2$	$p-1$	$S_b^2 = \frac{Q_b}{p-1}$
Interaction between a and b	$Q_c = n \sum_{i=1}^{k} \sum_{j=1}^{p} (\bar{X}_{ij.} - \bar{X}_{i..} - \bar{X}_{.j.} + \bar{X}_{...})^2$	$(k-1)(p-1)$	$S_c^2 = \frac{Q_c}{(k-1)(p-1)}$
Random error	$Q_e = \sum_{i=1}^{k} \sum_{j=1}^{p} \sum_{l=1}^{n} (X_{ijl} - \bar{X}_{ij.})^2$	$kp(n-1)$	$S_e^2 = \frac{Q_e}{kp(n-1)}$

k: number of groups, Effect a; p: number of groups, Effect b; n: sample size in for a given measuring profile, $\bar{X}_{i..}$: average of data in Group i for Effect a; $\bar{X}_{.j.}$: average of data in Group j for Effect b, $\bar{X}_{ij.}$: average of data for a given measuring profile, $\bar{X}_{...}$: average of all the measured data (k·p·n), X_{ijl}: any data in the dataset.

Water Practice & Technology Vol 16 No 2
doi: 10.2166/wpt.2021.006

At the given significance level, the result of the F-test indicates whether the difference between the examined groups exceeds the variation within the groups. For our PST data, a significance level of 99% was chosen to avoid Type-I error (rejection of a true null-hypothesis).

Two analyses were carried out using 2-way ANOVA with interaction (Table 3) at $q_{A1} = 5$ m h^{-1} (2i/1 and 2i/2). However, only one analysis was performed at $q_{A2} = 9.5$ m h^{-1} and at $q_{A3} = 13$ m h^{-1} each (2i/1). The effects a and b were used to analyse the dimensions of hydrodynamic flow characteristics (D), measurement reproducibility (R) and flow characteristic (FC). In Table 3, groups used for a given analysis are marked by ellipses/circles drawn with a continuous line. F-values are calculated and averaged for the data framed with a dashed line.

Effect a, 2i/1: Data were analysed to establish the reproducibility of measurements regarding flow components (Table 3). Data included in the analysis were measured for the same cross-section and at the same surface overflow rate, but on different days.

Effect b, 2i/1: Data were analysed to establish the dimension of hydrodynamic flow characteristics (Table 3). Data included in the analysis were the velocity components measured along the profiles of a given cross-section. Similar results are referred to as 2D, while different ones as 3D.

Effect a, 2i/2: Data were analysed to establish the reproducibility of measurements (Table 3). Data included in the analysis were measured for the same longitudinal section, but on different days.

Effect b, 2i/2: Data were analysed to characterize the flow developing in the PST. Data included in the analysis were the velocity components measured along the profiles of a given longitudinal section.

RESULTS AND DISCUSSION

Flow distribution

At a surface overflow rate of $q_{A1} = 5$ m h^{-1}, the flow pattern is strongly affected by high vertical velocity components ($w > 0.025$ m s^{-1}) (cross-section A in Figures 2 and 3) which stir up and dilute settled sludge in the sludge hopper and in the layer closest to the bottom. These components are generated by the design of the water inlet structure (lamellas positioned on the outer side of the inlet structure and directly in the settling zone as well as too low HRT in the inlet structure resulting in the insufficient dissipation of energy) and the jet flow developing along the tank. Results clearly indicate that kinetic and potential energy of the jet flow at the inlet need to be sufficiently dissipated within the inlet structure. For that, the design of the inlet structure should rely on hydrodynamic principles (satisfying the demands related to volume and HRT as well as optimal geometry).

Due to the concentration of suspended solids in the inflow and the much lower sludge mass stored in PSTs compared to that in the case of SSTs, the flow and transport processes of the already settled and thickened sludge mass do not affect the flow pattern considerably. Therefore, density effects in PSTs like the 'density waterfall' (Krebs 1991; Patziger 2007) in the inlet zone and density currents within the settling zone may be neglected (Figures 2 and 3).

In the examined PST, the distribution of velocity vectors in the longitudinal sections 2 and 4 were not homogenous (section 3 is located on the longitudinal axis of symmetry), in the first half of the tank (differences were particularly pronounced in the cross-sections A and B). Velocity vectors pointing backward (i.e. in the direction of the inlet point) are found in higher numbers in Profile A of section 2, while profile A of section 4 contains more vectors pointing forward (i.e. in the direction of the outlet point). Visual evaluation also confirmed a slightly asymmetric flow behaviour at a load of 5 m h^{-1} (Figures 2 and 3).

The 3D images of resultant velocity vectors are provided in Figure 3 where the effects of lateral velocity components are prominent already in the recommended nominal surface overflow range (1–4 m h^{-1}).

Water Practice & Technology Vol 16 No 2
doi: 10.2166/wpt.2021.006

Table 3 | 2-way ANOVA with interaction on PST data (groups used for a given analysis are marked by ellipses/circles drawn with a continuous line

Analysis	Effect	Description and method	Aim
2i/1	a	Comparison of flow features measured along all the profiles in a given cross-section on different days. The components u, v, w, Vm and TKE are considered separately. Groups are defined according to measuring days. F-values: 5 x 4 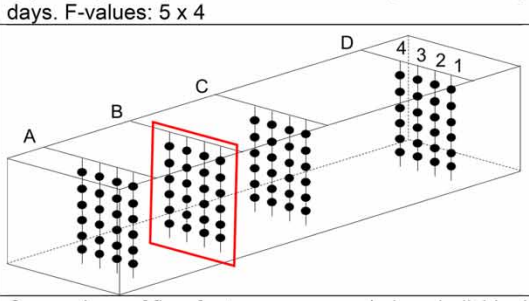	R
	b	Comparison of flow features measured along individual profiles in a given cross-section. The components u, v, w, Vm and TKE are considered separately. Groups are defined according to profiles within a single cross-section. F-values: 5 x 4. 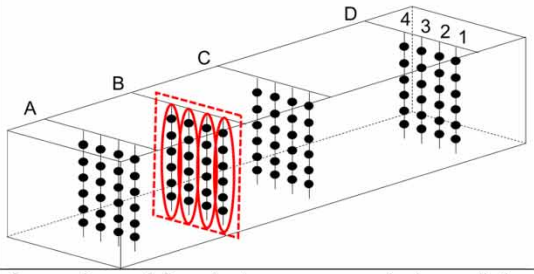	D
2i/2	a	Comparison of flow features measured along all the profiles in a given longitudinal section on different days. The components u, v, w, Vm and TKE are considered separately. Groups are defined according to measuring days. F-values: 5 x 4 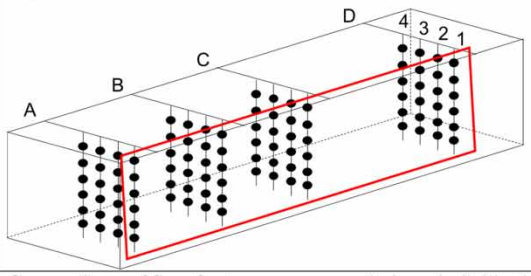	R
	b	Comparison of flow features measured along individual profiles in a given longitudinal section on different days. The components u, v, w, Vm and TKE are considered separately. Groups are defined according to profiles within a single longitudinal section. F-values: 5 x 4 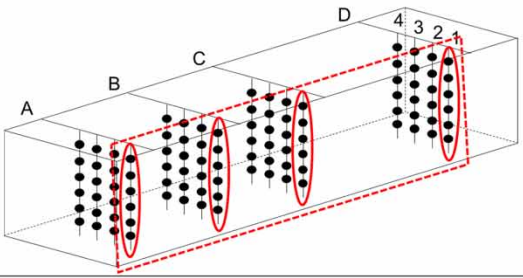	FC

F-values are calculated and averaged for the data framed with a dashed line.

The results of ANOVA for the reproducibility of measurements are symbolized by 'R+', if the data measured on a given day may be replaced by those from another measuring day and 'R−', if the data from different measuring days cannot replace each other.

Water Practice & Technology Vol 16 No 2
doi: 10.2166/wpt.2021.006

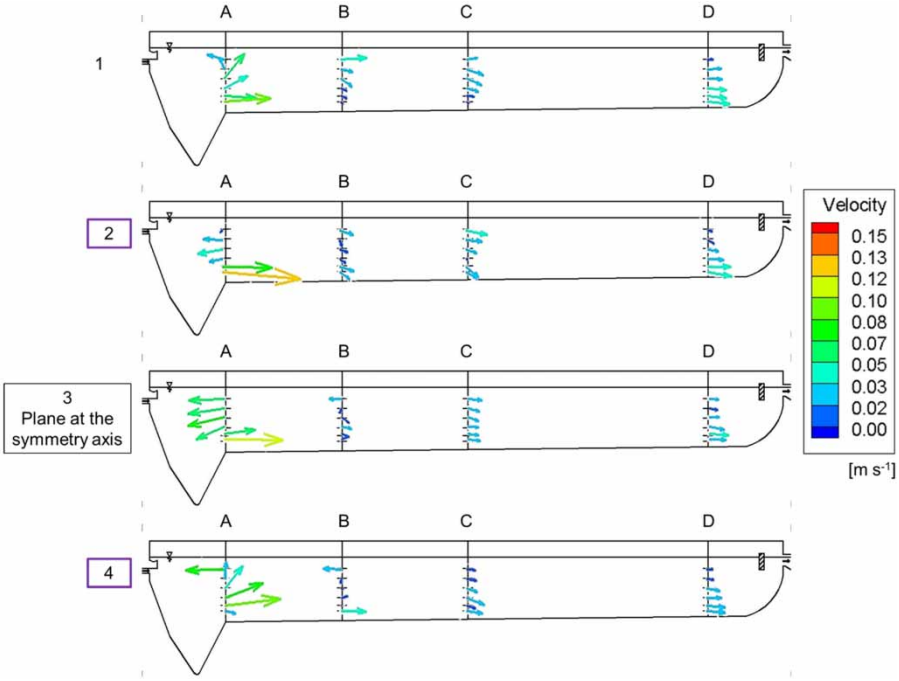

Figure 2 | Velocity distribution of the vectors of u-w in the four longitudinal sections at $q_{A1} = 5$ m h^{-1}. The cross-sections 2 and 4 (marked by purple frames) may be compared to the ones on opposite sides of the symmetry axis. The full colour version of this figure is available in the online version of this paper, at http://dx.doi.org/10.2166/wpt.2021.006.

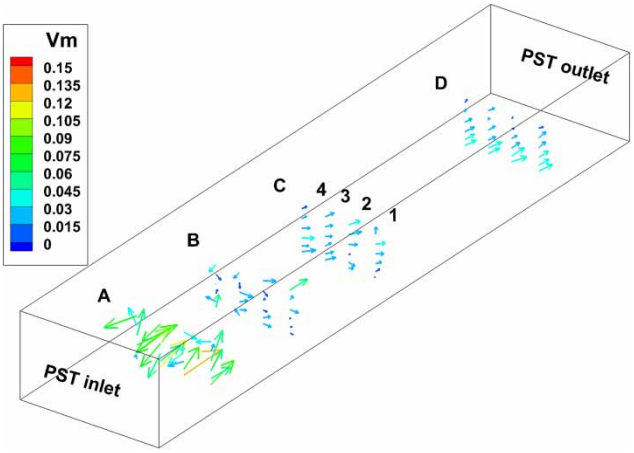

Figure 3 | 3D images of resultant velocity vectors [m s^{-1}] by $q_{A1} = 5$ m h^{-1}.

At surface overflow rates exceeding 5 m h^{-1}, the loads 9.5 and 13 m h^{-1} had higher impact on the flow field and the distributing effect of the inlet structure was more pronounced. Higher velocities and a more obvious upward pattern were observed near the inlet point at loads of 9.5 and 13 m h^{-1}. This phenomenon may result in the inflowing wastewater disturbing the already settled sludge near the sludge hopper. The flow pattern is strongly affected by high-velocity components induced by the design of the inlet structure (too low hydraulic retention time, lamellae), and the current developing along the tank (Patziger & Kiss 2015). While at a load of 9.5 m h^{-1} some small asymmetric currents were observed (Figures 4 and 5), at 13 m h^{-1} velocity vectors of extreme magnitude developed (Figures 6 and 7).

The 3D images of resultant velocity vectors for the rates 9.5 m h^{-1} and 13 m h^{-1} are presented in Figures 5 and 7, respectively. We may conclude that the higher the surface overflow rate, the larger the lateral velocity components become. This is caused by the flow distribution structure. For all

Water Practice & Technology Vol 16 No 2
doi: 10.2166/wpt.2021.006

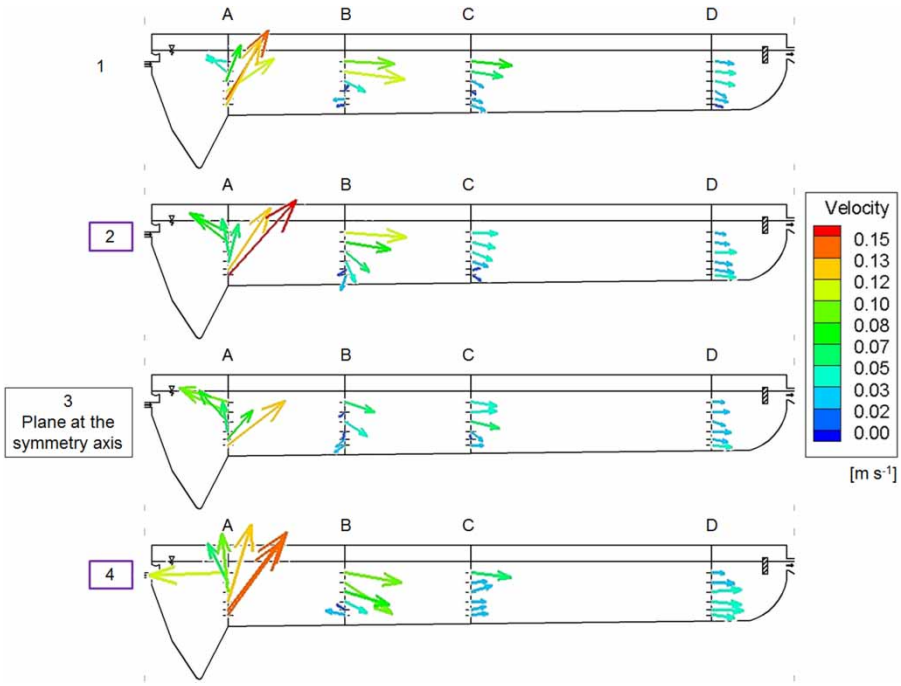

Figure 4 | Velocity distribution of the vectors u-w in the four longitudinal sections at $q_{A2} = 9.5$ m h^{-1} (the cross-sections 2 and 4 (marked by purple frames) may be compared as ones on opposite sides of the symmetry axis). The full colour version of this figure is available in the online version of this paper, at http://dx.doi.org/10.2166/wpt.2021.006.

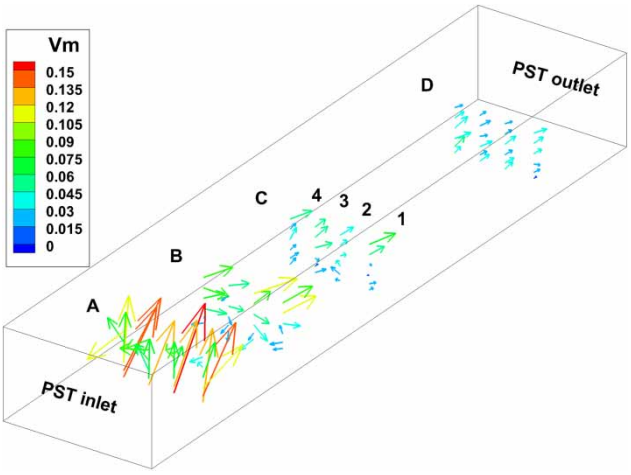

Figure 5 | 3D images of resultant velocity vectors [m s^{-1}] at $q_{A2} = 9.5$ m h^{-1}.

the three examined loads (5, 9.5 and 13 m h^{-1}), the volume facilitating efficient sedimentation is lower than that of the tank, as indicated by the vectors pointing upward and backward (in the direction of the inlet) typically occurring in the first third of the tank.

ANOVA

According to the results of ANOVA 2i/1, there was no interaction between the examined aspects regarding either velocity or turbulence (Figure 8). Averages stayed below the $F_{99\%}$ limit. Interaction (in the cases of w and TKE) could only be shown for cross-section B. This proves that values of the w-component measured on different days depended on the profiles where they were measured. The analysis of Effect a yielded no difference between the data measured on different days with

Water Practice & Technology Vol 16 No 2
doi: 10.2166/wpt.2021.006

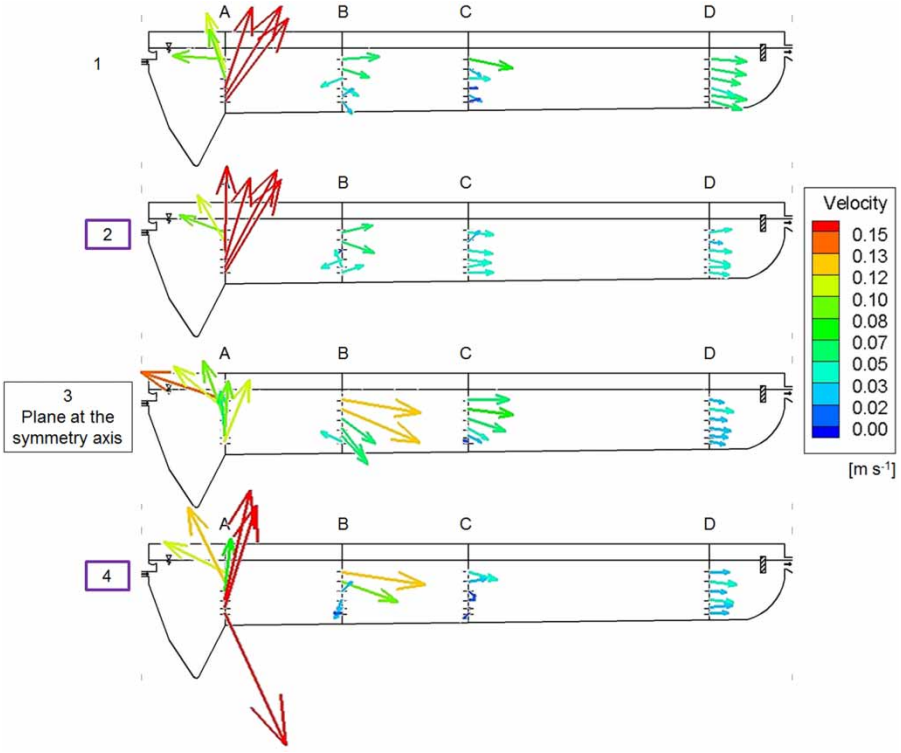

Figure 6 | Velocity distribution of the vectors of u-w in the four longitudinal sections at $q_{A3} = 13$ m h^{-1} (the cross-sections 2 and 4 (marked by purple frames) may be compared as ones on opposite sides of the symmetry axis). The full colour version of this figure is available in the online version of this paper, at http://dx.doi.org/10.2166/wpt.2021.006.

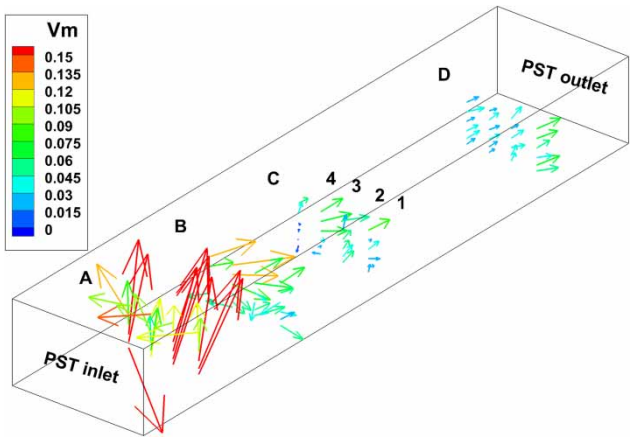

Figure 7 | 3D images of resultant velocity vectors [m s^{-1}] at $q_{A3} = 13$ m h^{-1}.

$F_{99\%}(2,66) = 4.94$ (20/20). Nevertheless, Fa values showed an increasing trend in the direction of the last cross-section (Figure 8). Thus, this measurement may be considered reproducible (R+). Similarly, based on the averages, no difference was found between the measuring profiles in a given cross-section at $F_{99\%}(3,66) = 4.10$ (15/20) with respect to Effect b (Figure 8). This means measurements as well as subsequent modelling may be performed in 2D with high certainty. Significant differences at $F_{99\%}$ could only be observed for cross-sections A and B, generated by w and TKE; and by u, w and TKE, respectively. Differences were apparent by the large velocity components and high turbulence that characterize the area in the vicinity of the inlet structure of the PST.

No interaction could be shown by the 2i/2 analysis for the data measured at 5 m h^{-1} (for F_{ab}-values, see Figure 9). Data measured on different days were similar at $F_{99\%}(2,66) = 4.94$ (20/20) (Effect a),

Water Practice & Technology Vol 16 No 2
doi: 10.2166/wpt.2021.006

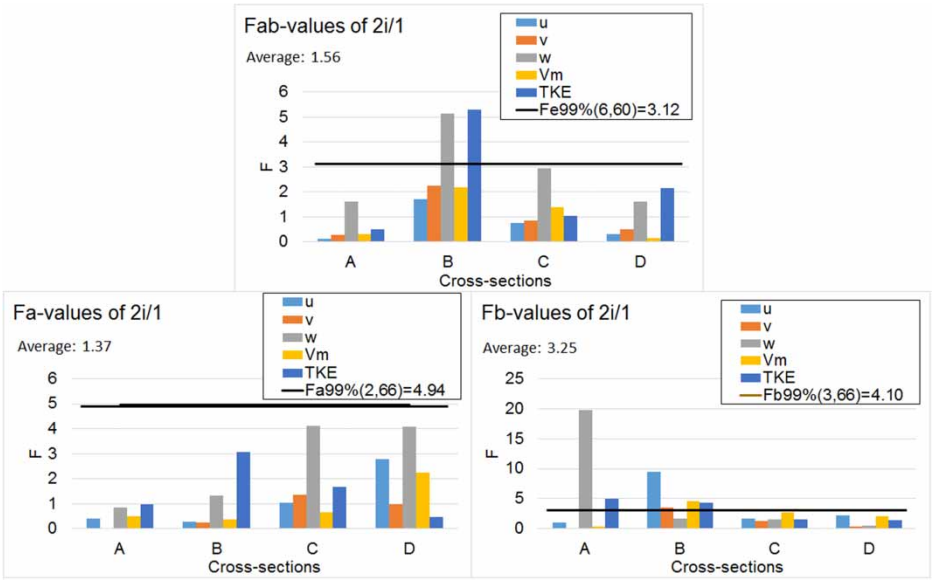

Figure 8 | Results of ANOVA 2i/1 for data measured at 5 m h^{-1}.

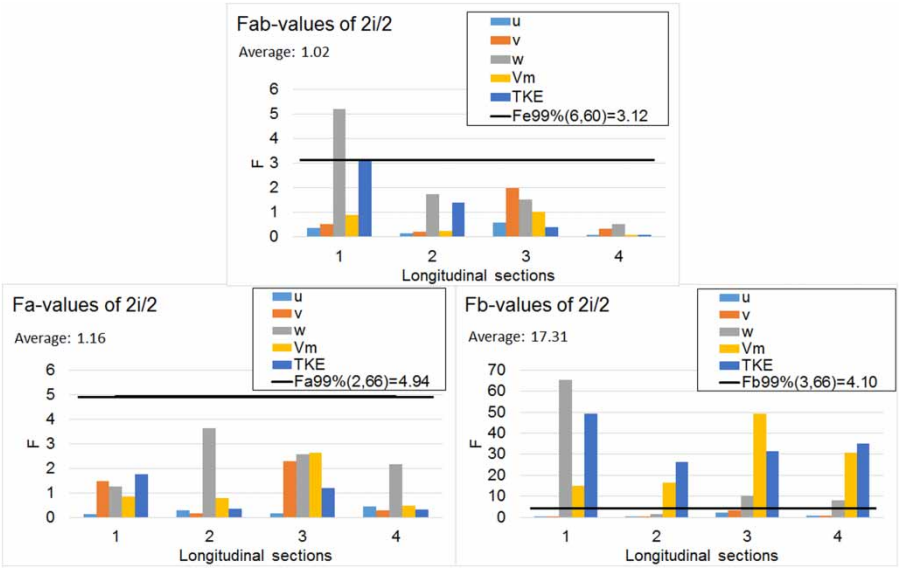

Figure 9 | Results of ANOVA 2i/2 at 5 m h^{-1}.

confirming reproducibility (R+). With respect to Effect b, a significant difference could be observed at $F_{99\%}(3,66) = 4.10$ (9/20) between the data measured in profiles within given longitudinal sections (Figure 9). High F-values were caused by the w component and thus F-statistics calculated for Vm and TKE exceeded the significance level in most cases. This result indicates that vertical velocity components changed along the PST and high vertical component values were present. Therefore, appropriate choice of distance is recommended between measurement points vertically.

The results of ANOVA at $q_{A1} = 5$ m h^{-1} are summarized in Table 4.

The results of 2i/1 ANOVA at $q_A = 9.5$ and 13 m h^{-1} indicated interactions related to the w component, TKE and u-component, Vm, TKE, respectively. Regarding the other data, no significant relationship could be shown between the effects. At 9.5 m h^{-1}, no significant difference was observed at $F_{99\%}(2,66) = 4$ regarding the average of Fa values at Effect a. However, w-component at cross-section A and TKE at cross-section D step over the significance level. Accordingly, flow features

Water Practice & Technology Vol 16 No 2
doi: 10.2166/wpt.2021.006

Table 4 | Summarized results of ANOVA at $q_{A1} = 5$ m h^{-1}

Method	Analysis No.	Effect	Aim	Results
2-way ANOVA with interaction	2i/1	a	R	R+
		b	D	No significant difference between profiles within a cross-section → 2D
	2i/2	a	R	R+
		b	FC	Vertical velocity component varies along the PST

measured on different days (R+) did not differ significantly. In the case of Effect b, data did not differ significantly at $F_{99\%}(3,66) = 4.1$ (Figure 10); that is, data measured along a vertical line were not significantly different within a given cross-section. Accordingly, we may conclude that clarifiers belonging to this type may be safety analysed by 2D methods (measuring, modelling). At the referred load, the w-component and TKE were significantly different at $F_{99\%}$ in the cross-sections A and D regarding Effect a. The data for the w component were significantly different at $F_{99\%}$ in cross-section B regarding Effect b.

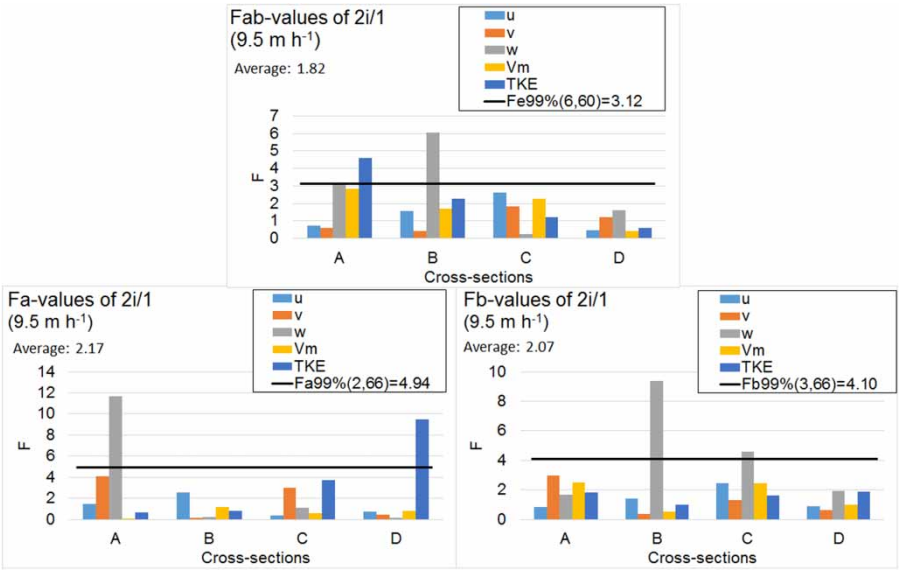

Figure 10 | Results of ANOVA 2i/1 at 9.5 m h^{-1}.

Data were less consistent at 13 m h^{-1}, but no interaction and no difference could be observed between velocity and TKE values measured on different days (Effect a: $F_{99\%}(2,66) = 1.882$) (Figure 11) (R+). Furthermore, the analyses of respective flow features regarding measuring profiles showed the similarity of data within one cross-section (Effect b: $F_{99\%}(3,66) = 3.913$) (Figure 11). Regarding Effect a, a significant difference could be observed at $F_{99\%}$, caused by the w component and TKE in cross-section A and B, respectively. F-values regarding Effect b showed a higher variance, significant at $F_{99\%}$, caused by the v-component, the w-component; u-component and Vm; and u-, w-component and Vm in the cross-sections A, B, C and D, respectively. Average differences between the data measured along different profiles in individual cross-sections stayed just below the significance level. Again, this result proves that measuring and modelling are possible using 2D methods; nevertheless, the application of a 3D measurement raster and 3D modelling also needs to be considered. It should be noted here that the turbulence developing at a surface overflow of 13 m h^{-1} requires spatial analysis.

Water Practice & Technology Vol 16 No 2
doi: 10.2166/wpt.2021.006

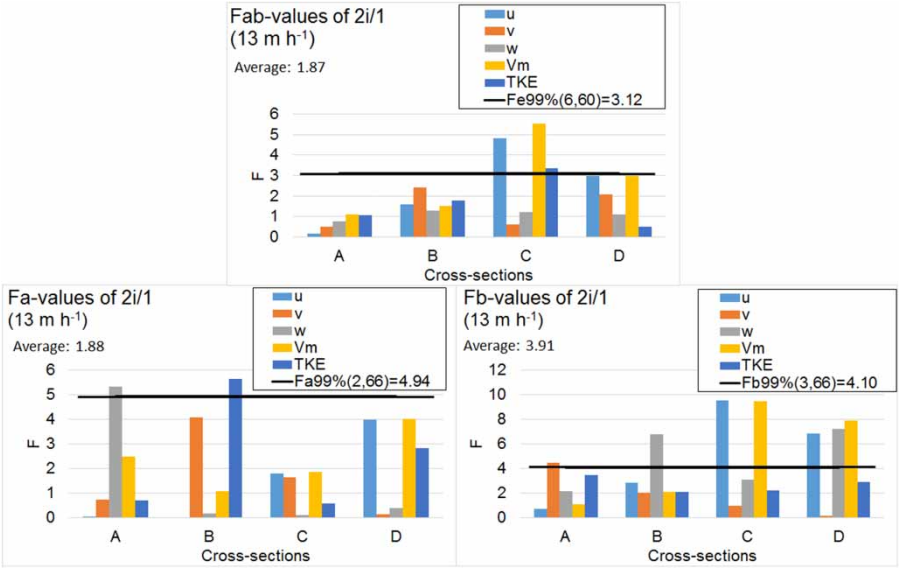

Figure 11 | Results of ANOVA 2i/1 at 13 m h^{-1}.

Results of ANOVA at $q_A = 9.5$ and 13 m h^{-1} are summarized in Table 5.

Table 5 | Summarized results of ANOVA at $q_A = 9.5$ and 13 m h^{-1}

Analysis No.	Effect	9.5 m h^{-1}	13 m h^{-1}
2i/1	a	R +	R +
	b	No significant difference between profiles within individual cross-sections → 2D	No significant difference between profiles within individual cross-sections → 2D possible, but 3D is recommended

CONCLUSIONS

Fine-scale flow measurement data in a PST were investigated innovatively by ANOVA to provide a decision support method for *in situ* measurement campaigns and further CFD modelling. (i) The spatial arrangement of measuring points to establish flow characteristics, (ii) measurement reproducibility and (iii) flow characteristics are determined quantitatively, considering several aspects.

(i) Spatial arrangement of measuring points to establish flow characteristics: the ANOVA analysis of repeated measurements showed no significant difference between profiles within individual cross-sections. Accordingly, 2D flow measuring and modelling methods are suitable for the analysis of this PST at $q_A = 5$ m h^{-1}, even at high overflow rates (9.5 m h^{-1}; 13 m h^{-1}). *Regarding practical applications, the longitudinal sections considered for the measurement campaigns of this type of PST should include one that comprises the hopper (and that single longitudinal section will suffice to provide the necessary data).* Such a campaign allows for the collection of sufficient information about the prevalent wastewater flow features inside the tank.

(ii) Reproducibility of measurements: Measurements may be consistently reproduced under the same initial and boundary conditions, because flow characteristics inside the PST measured at different days do not differ significantly. Accordingly, *the second practical consideration is that in rectangular PSTs, a single measurement campaign may suffice* to collect the necessary information about flow characteristics. Avoiding unnecessary repetitions saves time, effort and cost.

(iii) Flow characteristics: The vertical inhomogeneity of data within individual profiles was mostly observed in the vicinity of the inlet structure of the PST. The vertical variation in velocity

Water Practice & Technology Vol 16 No 2
doi: 10.2166/wpt.2021.006

values implies *a third practical consideration; that is, that the raster points selected for measuring within a single profile should not be spaced further than 0.5 m apart. Furthermore, near the bottom, the distance between points should not exceed 0.3 m*. It is strongly advised to measure a higher number of cross-sections near the inlet of rectangular PSTs where the turbulence is higher, to obtain sufficient information about flow conditions, so that a detailed picture may be developed about the conditions at the inlet structures of PSTs.

Relying on the data thus collected, a simplified CFD model may be set for further measurement campaigns in similar PSTs, thus reducing computing time and effort.

DECLARATIONS OF INTEREST

None.

ACKNOWLEDGEMENT

The authors would like to thank the employees of Graz Municipal Wastewater Treatment Plant and the University of Technology Graz for their assistance and Marianna Bolla, D.Sc., habilitated Associate Professor (Department of Stochastics of the Budapest University of Technology and Economics) for her help in performing the statistical analysis.

DATA AVAILABILITY STATEMENT

Data cannot be made publicly available readers should contact the corresponding author for details.

REFERENCES

Alleyne, A. A., Xanthos, S., Ramalingam, K., Temel, K., Li, H. & Tang, H. S. 2014 Numerical investigation on flow generated by Invent mixer in full-scale wastewater stirred tank. *Engineering Applications of Computational Fluid Mechanics* **8**(4), 503–517. https://doi.org/10.1080/19942060.2014.11083303.

ATV-DVWK A 131 2016 *Standard, Bemessung von einstufigen Belebungsanlagen (Dimensioning of Single-Stage Activated Sludge Plants)*. GFA Publishing Company of ATV-DVWK, Hennef, Germany (in German).

Bolla, M. & Krámli, A. 2005, 2012 Statisztikai következtetések elmélete (Theory of statistical inference), 1st and 2nd edn. *Typotex* (in Hungarian).

Burt, D. J. 2010 *Improved Design of Settling Tanks Using an Extended Drift Flux Model*. Dissertation, University of Bristol, Bristol, UK.

Das, S., Bai, H., Wu, C., Kao, J.-H., Barney, B., Kidd, M. & Kuettel, M. 2016 Improving the performance of industrial clarifiers using three-dimensional computational fluid dynamics. *Engineering Applications of Computational Fluid Mechanics* **10**(1), 130–144. https://doi.org/10.1080/19942060.2015.1121518.

Ekama, G. & Marais, P. 2000 *Hydrodynamic Modelling of Secondary Settling Tanks*. *WRC Report* No. 835/1/02 Part 1. WRC, Swindon, UK.

Gao, H. & Stenstrom, M. K. 2018 Evaluation of three turbulence models in predicting the steady state hydrodynamics of a secondary sedimentation tank. *Water Research* **143**, 445–456. https://doi.org/10.1016/j.watres.2018.06.067.

Gao, H. & Stenstrom, M. K. 2019a The influence of wind in secondary settling tanks for wastewater treatment – a computational fluid dynamics study. Part I: circular secondary settling tanks. *Water Environment Research*. https://doi.org/10.1002/wer.1241

Gao, H. & Stenstrom, M. K. 2019b The influence of wind in secondary settling tanks for wastewater treatment – a computational fluid dynamics study. Part II: rectangular secondary settling tanks. *Water Environment Research* **92**(4), 541–550. https://doi.org/10.1002/wer.1244

Gregušová, V., Škultétyová, I. & Holubec, M. 2017 Measurement of flow velocity in different secondary settling tanks for analysis of the flow. *Pollack Periodica* **12**(3), 15–22. https://doi.org/10.1556/606.2017.12.3.2.

Imam, E. H. 1981 *Numerical Modelling of Rectangular Clarifiers*. Dissertation. University of Windsor, Ontario, Canada.

Water Practice & Technology Vol 16 No 2
doi: 10.2166/wpt.2021.006

Imam, E., McCorquodale, J. A. & Bewtra, J. K. 1983 Numerical modelling of sedimentation tanks. *Journal of Hydraulic Engineering* **109**(12), 1740–1754.

Karpinska, A. M. & Bridgeman, J. 2016 CFD-aided modelling of activated sludge systems – a critical review. *Water Research* **88**, 861–879. http://dx.doi.org/10.1016/j.watres.2015.11.008.

Karpinska, A. M. & Bridgeman, J. 2017 Towards a robust CFD model for aeration tanks for sewage treatment – a lab-scale study. *Engineering Applications of Computational Fluid Mechanics* **11**(1), 371–395. https://doi.org/10.1080/19942060.2017.1307282.

Kemper, M. 2016 *Strömungsverhalten und Sedimentationswirksamkeit in Regenbecken mit Schrägklärer-Einbauten (Flow Behaviour and Sedimentation Effectiveness in Stormwater Retention Tank with Clarifier with Lamellae)*. Dissertation, Karlsruher Instituts für Technologie, Karlsruhe, Germany (in German).

Kiss, K. 2013 On settling process in primary clarifiers. In *Second Conference of Junior Researchers in Civil Engineering*, Budapest, Hungary.

Kiss, K. & Patziger, M. 2018 On the accuracy of three dimensional flow measurements at low velocity ranges in municipal wastewater treatment reactors. *Flow Measurement and Instrumentation* **64**, 39–53. https://doi.org/10.1016/j.flowmeasinst.2018.10.002.

Krebs, P. 1991 The hydraulics of final settling tanks. *Water Science and Technology* **23**(4–6), 1037–1046.

Larsen, P. 1977 *On the Hydraulics of Rectangular Settling Basins, Experimental and Theoretical Studies, Department of Water Resources Engineering, Lund Institute of Technology University of Lund, Report No. 1001*. Lund, Sweden.

Lindeborg, C., Wiberg, N. & Seyf, A. 1996 Studies of the dynamic behaviour of a primary sedimentation tank. *Water Science and Technology* **34**(3–4), 213–222. doi:10.2166/wst.1996.0435.

Mazzolani, G., Pirozzi, F. & d'Antonio, G. 1998 A generalized settling approach in the numerical modelling of sedimentation tanks. *Water Science and Technology* **38**(3), 95–102. https://doi.org/10.1016/S0273-1223(98)00453-3.

Nortek AS 2005 *Vector Current Meter, User Manual*. Nortek, Rud, Norway.

Patziger, M. 2007 *Untersuchung der Schlammbilanz in Belebungsstufenaufbauend auf den Prozessenim Nachklärbecken. Schriftenreihezur Wasserwirtschaft (Investigation of the Sludge Balance in Activated Stages Based on the Secondary Sludge Tank Processes)*. Dissertation, Graz University of Technology, Graz, Austria (in German).

Patziger, M. & Kiss, K. 2015 Towards a hydrodynamically enhanced design and operation of primary settling tanks – results of a long term in situ measurement investigation program. *Water Environment Journal* **29**(3), 338–345. https://doi.org/10.1111/wej.12125.

Patziger, M., Kainz, H., Józsa, J. & Hunze, M. 2005 Messung und Modellierung von physikalischen Prozessen in Nachklärbecken (Measurement and modeling of physical processes in secondary clarifiers). *Österreichische Wasser und Abfallwirtschaft* **57**(12/05), 177–184. (in German).

Patziger, M., Kainz, H., Hunze, M. & Józsa, J. 2012 Influence of secondary settling performance on suspended solids mass balance in activated sludge systems. *Water Research* **46**(7), 2415–2424. https://doi.org/10.1016/j.watres.2012.02.007.

Ramin, E., Wágner, D. S., Yde, L., Binning, P. J., Rasmussen, M. R., Mikkelsen, P. S. & Plósz, B. G. 2014 A new settling velocity model to describe secondary sedimentation. *Water Research* **66**, 447–458. https://doi.org/10.1016/j.watres.2014.08.034.

Razmi, A., Firoozabadi, B. & Ahmadi, G. 2009 Experimental and numerical approach to enlargement of performance of primary settling tanks. *Journal of Applied Fluid Mechanics* **2**(1), 1–12.

Rostami, F., Shahrokhi, M., Said, M. A. M., Abdullah, R. & Syafalni, S. 2011 Numerical modeling on inlet aperture effects on flow pattern in primary settling tanks. *Applied Mathematical Modelling* **35**(6), 3012–3020. https://doi.org/10.1016/j.apm.2010.12.007.

Shahrokhi, M., Rostami, F., Said, M. A. M., Yazdi, S. R. S. & Syafalni, 2012 The effect of number of baffles on the improvement efficiency of primary sedimentation tanks. *Applied Mathematical Modelling* **36**(8), 3725–3735. https://doi.org/10.1016/j.apm.2011.11.001.

Shahrokhi, M., Rostami, F., Said, M. A. M. & Syafalni, 2013 Numerical modelling of baffle location effects on the flow pattern of primary sedimentation tanks. *Applied Mathematical Modelling* **37**(6), 4486–4496. https://doi.org/10.1016/j.apm.2012.09.060.

Skáfár, B., Péter, N. & Kristóf, G. 2016 Rothasztó tornyok CFD modellezése (CFD modelling of digesters). In *III. Soós Ernő Scientific Conference: Water- and Wastewater Treatment in Industry (VSZI'16)*, Nagykanizsa, Hungary (in Hungarian).

Valle Medina, M. E. & Laurent, J. 2020 Incorporation of a compression term in a CFD model based on the mixture approach to simulate activated sludge sedimentation. *Applied Mathematics* **77**, 848–860.

Wicklein, E. A. & Samstag, R. W. 2008 Comparing commercial and transport CFD models for secondary sedimentation. In *Conference Paper*, Water Environment Federation, December 2008. https://doi.org/10.2175/193864709793952765.

Winkler, K. 2001 Räumung in Nachklärbecken von Abwasserreinigungsanlagen (Scrape in secondary clarifiers at wastewater treatment plants). *Research project*, Versuchsanstalt für Wasserbau Hydrologie und Glaziologie der Eidgenössischen Technischen Hochschule Zürich, Switzerland.

First received 29 September 2020; accepted in revised form 24 January 2021. Available online 4 February 2021